Temperature Dependence of Cation Distribution and Oxidation State in Magnetic Mn−Fe Ferrite Nanocrystals

Z. John Zhang,*,† Zhong L. Wang,‡ Bryan C. Chakoumakos,§ and Jin S. Yin‡

Contribution from the School of Chemistry & Biochemistry and School of Materials Science & Engineering, Georgia Institute of Technology, Atlanta, Georgia 30332-0400, and Solid State Division, Oak Ridge National Laboratory, Oak Ridge, Tennessee 37831-6393

Received September 2, 1997

Abstract: The magnetic properties of spinel nanoparticles are determined by crystal chemistry issues such as cation distribution and oxidation states. The cation distribution and oxidation state of Mn−Fe spinel nanoparticles have been systematically studied at various temperatures by using neutron diffraction and electron energy loss spectroscopy, respectively. The Mn−Fe spinel nanoparticles prepared by coprecipitation have a high degree of inversion with 61% of the tetrahedral sites occupied by Fe^{3+} cations. The degree of inversion correlates with the distribution expected from random occupancy of cations consisting of Fe (60%) and Mn (40%). After heat treatment in a vacuum, the cation distribution reaches an equilibrium state with a 29% inversion. Initially, one-half of the Mn cations are in the +3 oxidation state and the other half are in the +2 oxidation state. Mn^{3+} cations are slowly and irreversibly reduced to Mn^{2+} with increasing temperature. When the temperature approaches 600 °C, all Mn cations are in the +2 state. These results provide direct evidence for the temperature-dependent change of crystal chemistry in Mn−Fe spinel nanoparticles, which has been closely related with the controversy on attributing the changes in the magnetic properties of the nanoparticles to crystallite size effect. These results will also provide an understanding of how to control crystal chemistry in order to control the properties of these magnetic nanoparticles.

Introduction

Magnetic nanoparticles of spinel ferrites are of great interest in fundamental science such as for addressing the fundamental relationships between magnetic properties of nanoparticles and their crystal chemistry and structure. They also have potential applications such as contrast agents in magnetic resonance imaging (MRI).[1] Due to their reduced sizes, these nanoparticles may possess novel and/or improved properties in comparison to the bulk materials, which have been extensively used in electronic devices for high-frequency telecommunications.[2] For instance, $CdFe_2O_4$ nanoparticles with a size of about 8 nm have displayed enhanced magnetization.[3] A clear understanding of the crystal chemistry of spinel nanoparticles is essential for studying and controlling their magnetic properties, because of the relative complexity of spinel oxide compounds and close connections between their magnetic properties and their crystal chemistry and structures.[3−8]

Over the past few years, $MnFe_2O_4$ spinel ferrite nanoparticles have attracted considerable attention.[9] $MnFe_2O_4$ has a face-centered cubic structure with two types of cation lattice sites: (1) a tetrahedral lattice site A formed by four oxygen anions, and (2) an octahedral lattice site B formed by six oxygen anions (Figure 1). There are 8 A sites and 16 B sites in each unit cell. The percentage of the A sites occupied by Fe species determines the degree of inversion with 100% occupancy of A sites by Fe species and Mn species corresponding to 100% inversion and zero inversion, respectively. The magnetic properties are closely related to the inversion degree since the $Fe^{3+}{}_A-Fe^{3+}{}_B$ superexchange interaction is much stronger than the $Mn^{2+}{}_A-Fe^{3+}{}_B$ interaction.[6,10] The magnetic properties such as Curie transition temperature in nanoparticles prepared by coprecipitation have been noted to change as the particle size changes.[11−13] However, there is considerable controversy about the origin of these reported changes partially due to the uncertainty in the crystal chemistry of these nanoparticles.[14−17] In bulk spinel compounds, the crystal chemistry and structure, mainly the cation

* To whom correspondence should be addressed.
† School of Chemistry & Biochemistry.
‡ School of Materials Science & Engineering.
§ Oak Ridge National Laboratory.

(1) Saini, S.; Stark, D. D.; Hahn, P. F. *Radiology* **1987**, *162*, 217.
(2) Wohlfarth, E. P., Ed. *Ferromagnetic Materials*; North-Holland: Amsterdam, 1980; Vol. 2, Chapters 3 and 4.
(3) Yokoyama, M.; Sato, T.; Ohta, E.; Sato, T. *J. Appl. Phys.* **1996**, *80*, 1015.
(4) Verwey, E. J. W.; Heilmann, E. L. *J. Chem. Phys.* **1947**, *15*, 174.
(5) Harrison, F. W.; Osmond, W. P.; Teale, R. W. *Phys. Rev.* **1957**, *106*, 865.
(6) Van Groenou, A. B.; Bongers, P. F.; Stuyts, A. L. *Mater. Sci. Eng.* **1968**/**69**, *3*, 317.
(7) Van der Zaag, P. J.; Johnson, M. T.; Noordermeer, A.; Por, P. T.; Rekveldt, M. T. *J. Magn. Magn. Mater.* **1991**, *99*, L1.
(8) Kamiyama, T.; Haneda, K.; Sato, T.; Ikeda, S.; Asano, H. *Solid State Commun.* **1992**, *81*, 563.
(9) Gillot, B.; Laarj, M.; Kacim, S. *J. Mater. Chem.* **1997**, *7*, 827 and references therein.
(10) Goodenough, J. B.; Loeb, A. L. *Phys. Rev.* **1955**, *98*, 391.
(11) Tang, Z. X.; Sorensen, C. M.; Klabunde, K. J.; Hadjipanayis, G. C. *Phys. Rev. Lett.* **1991**, *67*, 3602.
(12) Kulkarni, G. U.; Kannan, K. R.; Arunarkavalli, T.; Rao, C. N. R. *Phys. Rev. B* **1994**, *49*, 724.
(13) Chen, J. P.; Sorensen, C. M.; Klabunde, K. J.; Hadjipanayis, G. C.; Devlin, E.; Kostikas, A. *Phys. Rev. B* **1996**, *54*, 9288.
(14) Van der Zaag, P. J.; Noordermeer, A.; Johnson, M. T.; Bongers, P. F. *Phys. Rev. Lett.* **1992**, *68*, 3112.
(15) Brabers, V. A. M. *Phys. Rev. Lett.* **1992**, *68*, 3113.
(16) Tang, Z. X.; Chen, J. P.; Sorensen, C. M.; Klabunde, K. J.; Hadjipanayis, G. C. *Phys. Rev. Lett.* **1992**, *68*, 3114.
(17) Van der Zaag, P. J.; Brabers, V. A. M.; Johnson, M. T.; Noordermeer, A.; Bongers, P. E. *Phys. Rev. B* **1995**, *51*, 12009.

S0002-7863(97)03085-0 CCC: $15.00
Published on Web 02/05/1998

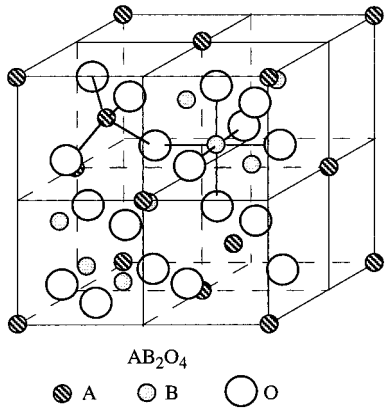

Figure 1. The unit cell of the spinel structure with half of the A and B sites shown.

distribution and oxidation state are the determining factors for the magnetic properties.[6] The cation distribution and oxidation state are uncertain in the nanoparticles used in size-effect studies. The changes of magnetic properties such as Curie transition temperature could be due to different crystal chemistry among these nanoparticles. The cation distribution in the nanoparticles has been studied with Mössbauer spectroscopy;[12,13] however, the presumption of the same recoilless fractions for Fe^{3+} in tetrahedral and octahedral sites usually causes concern of accuracy in Mössbauer data analysis.[18] The oxidation state of Mn in these Mn−Fe spinel ferrite nanoparticles has only been speculated due to the lack of adequate experimental results.[13,17] Clearly, an unambiguous understanding of the cation distribution and oxidation state in $MnFe_2O_4$ nanoparticles is required for the study of their magnetic properties, especially the widely concerned particle-size effects in the magnetic nanoparticles.

We herein report the studies on the oxidation state and the cation distribution of the nanoparticles prepared by coprecipitation using electron energy loss spectroscopy (EELS) and neutron powder diffraction, respectively. As-prepared magnetic nanoparticles have a high degree of inversion in the cation distribution, and the cation distribution changes drastically after the nanoparticles are heated in a vacuum. Mn species have a mixed valence of +2 and +3 in as-prepared nanoparticles. As the nanoparticles are heated in a vacuum, the in-situ EELS studies show that all the Mn^{3+} cations are eventually converted to Mn^{2+} cations.

Our studies demonstrate that the crystal chemistry of Mn−Fe spinel nanoparticles can change greatly depending upon the annealing conditions. Therefore, the magnetic properties of Mn−Fe spinel nanoparticles such as Curie transition temperature may vary considerably with different annealing conditions even in the same spinel nanoparticle system. Our results suggest that the shift of Curie transition temperature in Mn−Fe spinel nanoparticles, previously attributed to crystallite size effect, may be due to annealing-induced changes in cation distribution and oxidation state. A well-defined crystal chemistry in Mn−Fe spinel nanoparticles is essential for a valid conclusion on the particle size effect to the magnetic properties of the nanoparticles.

(18) Long, G. J. in *Mössbauer Spectroscopy Applied to Inorganic Chemistry*; Long, G. J., Ed.; Plenum: New York, 1984; Vol. 1, p 7.

Experimental Section

Nanoparticle Preparation. The Mn−Fe spinel nanoparticles were prepared with the coprecipitation method.[19] The starting materials, $FeCl_3 \cdot 6H_2O$ and $MnCl_2 \cdot 4H_2O$ solids, were dissolved in water with the concentrations of 0.8 and 0.4 M, respectively. The aqueous mixture of $MnCl_2$ and $FeCl_3$ was slowly poured into a magnetically stirred 6 M NaOH solution, and the molar ratio of the total metal cation concentration [M] and [OH^-] was 0.2. A precipitate was formed, and the slurry was then placed in a boiling water bath to digest for 2 h. After the digestion, the slurry was filtered and washed until the pH in the solution became neutral. The particles obtained were dried in air at 145 °C for 2 h.

Neutron Diffraction. Neutron diffraction data were collected with use of the HB4 powder diffractometer at the High-Flux Isotope Reactor at Oak Ridge National Laboratory. The sample was placed in a vanadium can for data collection at 25 °C over the 2-θ range of 11° to 135° in steps of 0.05°. The wavelength was precisely determined to be 1.0911(1) Å on the basis of the refinements of Si standard. An array of 32 equally spaced (2.7°) ^{3}He detectors can be step-scanned over a range of up to 40°. The data were corrected for the variation in detector efficiencies, which were determined by using a vanadium standard. For high-temperature measurements, a vacuum furnace with a niobium heating element was used. The sample temperature in the furnace was calibrated by using the thermal expansion of magnesium oxide. The nuclear and magnetic structures of the sample were refined by using the General Structure Analysis System (GSAS) program.[20] The pseudo-Voigt peak-profile function truncated at 0.3% of the peak height was used, including two refinable terms for the Lorentzian portion.[21] Peak asymmetry was refined, and the intensities were corrected for the Lorentz effect. The background was approximated by a cosine Fourier series with four terms.

EELS Studies. The EELS experiments were performed with a Hitachi HF-2000 field-emission transmission electron microscope with a Gatan 666 parallel detector. A Gatan 628 TEM specimen heating stage was employed to conduct the in-situ temperature-dependent EELS experiments. The specimen temperature can be increased continuously from room temperature to 1000 °C. The sample chamber column pressure was kept at 3×10^{-8} Torr or lower even during the heating. The EELS spectra were acquired in the image mode at a magnification of 40000−100000. The nanoparticles were dispersed on holey carbon grids for TEM observation, and the EELS spectra were recorded consecutively from the same specimen region. The low-energy-loss spectrum from the valence shell was used to remove the multiple-inelastic-scattering effect in the core-loss region by using the Fourier ratio technique.[22] Therefore, the spectra presented here are the results of the single scattering of electrons.

Results and Discussion

Mn−Fe Spinel Nanoparticle Formation. X-ray diffraction studies showed that the sample was a pure spinel phase with no impurity peaks (Figure 2). The electron diffraction pattern also matched with the cubic spinel structure (inset in Figure 3). We determined the size of nanoparticles in two ways. First, from analysis of the diffraction peak broadening with use of the Scherrer equation, the particles had a size of about 40 nm. Second, high-resolution transmission electron microscopy (HRTEM) studies confirmed that the size of these nanoparticles was about 40 nm and was fairly uniform as shown in Figure 3. The consistent results on the nanoparticle size from X-ray diffraction and transmission electron microscopy (TEM) ob-

(19) Tang, Z. X.; Sorensen, C. M.; Klabunde, K. J.; Hadjipanayis, G. C. *J. Colloid Interface Sci.* **1991**, *146*, 38.

(20) Larson, A. C.; von Dreele, R. B. GSAS-General Structure Analysis System; Rept. LA.-UR-86-748, Los Alamos National Laboratory, Los Alamos, 1989.

(21) Thompson, P.; Cox, D. E.; Hastings, J. B. *J. Appl. Crystallogr.* **1987**, *20*, 79.

(22) Egerton, R. F. *Electron Energy-Loss Spectroscopy in the Electron Microscope*, 2nd ed.; Plenum Press: New York, 1996.

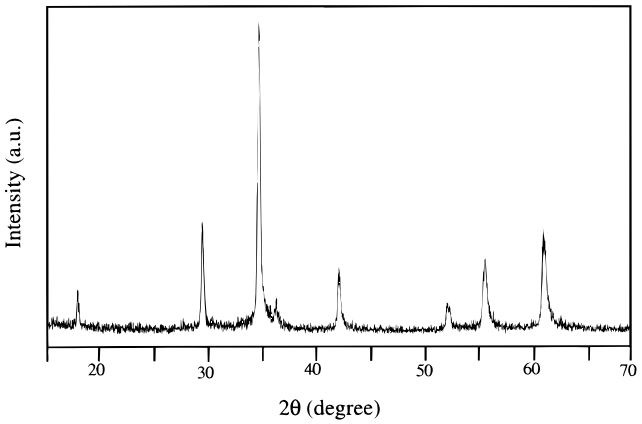

Figure 2. X-ray diffraction pattern (Cu Kα radiation) of Mn−Fe ferrite spinel nanoparticles.

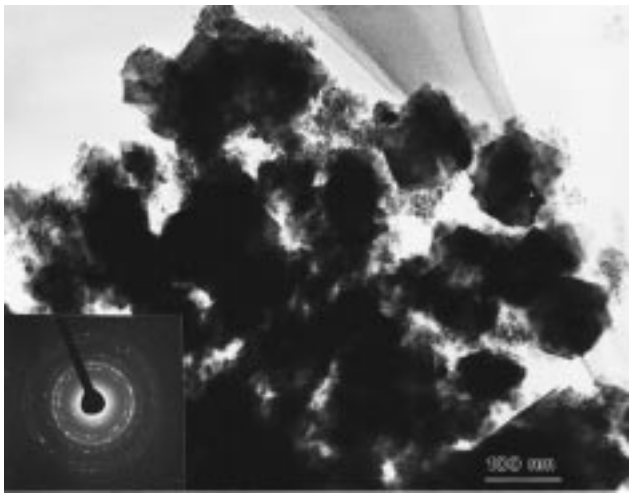

Figure 3. Transmission electron micrograph of Mn−Fe ferrite spinel nanoparticles (about 40 nm in size). The inset shows the electron diffraction pattern of these nanoparticles with the cubic spinel structure.

servations imply that the sample consists of single-crystal nanocrystals. After the heat treatment, the particle size remained unchanged. Although the accurate chemical composition of the sample is not crucial to our discussion here, the [Mn]/[Fe] ratio in the sample was analyzed by using ICP technique, which suggested a ratio of about 0.6, well in the range common for the Mn−Fe spinel compositions.

Cation Distribution. Neutron powder diffraction was employed to determine the cation distribution in these Mn−Fe spinel nanoparticles. Because the coherent neutron scattering lengths for Fe and Mn differ significantly (0.954×10^{-12} and -0.373×10^{-12} cm, respectively), neutron diffraction is an ideal technique for the precise determination of the cation distribution in $MnFe_2O_4$ spinel nanoparticles.[23,24] The temperature dependence of the Fe/Mn cation distribution in the nanoparticles was systematically studied by in-situ data collection in a vacuum furnace at 25, 363, and 485 °C and back to 25 °C. The cation distribution at various temperatures was obtained by whole-pattern fitting with use of the Rietveld method. Figure 4 displays the neutron diffraction patterns and fits to data obtained at 25 °C before and after the heating cycle. The fractions of Mn and Fe on both A and B sites were refined, and the individual A and B site magnetic moments were also refined. The oxygen content was not refined due to the relatively weak

(23) Hastings, J. M.; Corliss, L. M. *Phys. Rev.* **1956**, *104*, 328.
(24) Sakurai, J.; Shinjo, T. *J. Phys. Soc. Jpn.* **1967**, *23*, 1426.

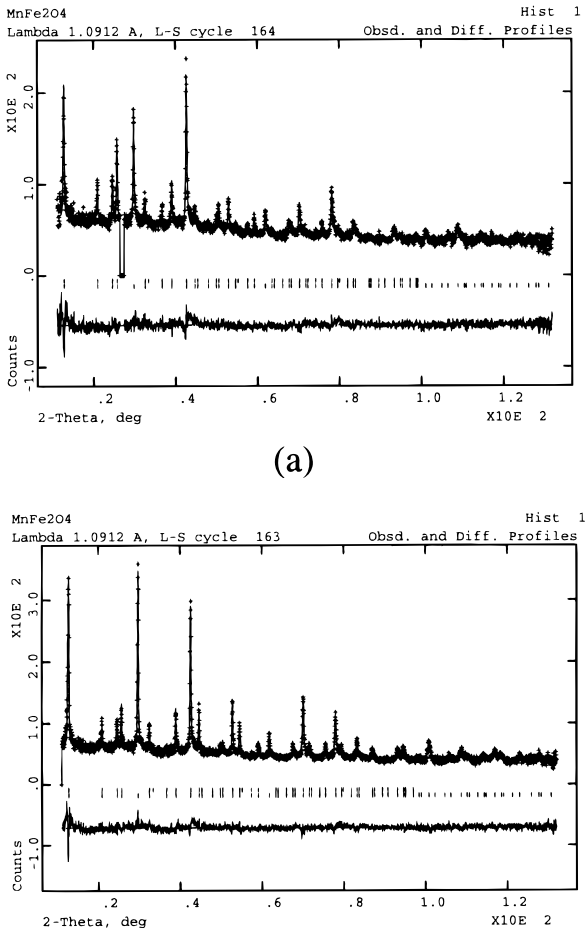

Figure 4. Neutron diffraction patterns ($\lambda = 1.0911$ Å) of Mn−Fe ferrite spinel nanoparticles at 25 °C (a) before vacuum heating and (b) after vacuum heating. The "goodness of fit", χ^2, for these two patterns is 1.26 and 1.37, respectively. Below the pattern, the first row of the sticks mark the peaks from the magnetic scattering, and the second row of the sticks correspond to the peaks from the nuclear scattering. The excluded region near $2\theta = 30°$ in spectrum eliminates the 110 diffraction peak of the Nb heating element of the furnace.

diffraction intensity. The results from the refinement of the neutron diffraction data are displayed in Table 1.[25]

The cation distribution apparently reaches its equilibrium state after the heating in a vacuum. The neutron diffraction study at 25 °C on as-prepared nanoparticles (Figure 4a) shows that the inversion degree is as high as 61% for Fe at the A sites. The Rietveld refinement results suggest a formula for as-prepared nanoparticles as $Mn_{0.39}Fe_{0.61}(Mn_{0.82}Fe_{1.18})O_4$ where cations in the brackets occupy the B sites. The magnetic scattering can only be observed at low Bragg angles (Figure 4). The diffraction peaks at $2\theta \sim 33$, 55, and 79 are purely from the magnetic scattering. Such peaks originate from the antiferromagnetic order possessed by the nuclear structure. This is consistent with the well-studied antiferromagnetic ordering in bulk Mn−Fe spinel materials.[26] For the data collected at 363

(25) The precision of ±0.01 from the least-squares fit is clearly overestimated, because the total Mn and Fe compositions from these fits vary from 1.13 to 1.21 and from 1.79 to 1.86, respectively, over the four heat treatments. Since the vacuum heating should not change the cation compositions, the more realistic error estimates would be 7 to 8 times as large in data fits, and thus there is no significant difference among the results obtained at 363, 485, and 25 °C (after heating).
(26) Wohlfarth, E. P., Ed. *Ferromagnetic Materials*; North-Holland: Amsterdam, 1982; Vol. 3, Chapter 4.

Table 1. Structural Parameters from Rietveld Refinements of Neutron Powder Diffraction Data for a Nanocrystalline $(Mn,Fe)(Mn,Fe)_2O_4$ Spinel

measurement order	T (°C)	cell edge a (Å)	site occupancies[a]		x(O)	isotropic displacement parameters			moments		agreement factors	
			A-site	B-site		$U(A)$ (Å^2)	$U(B)$ (Å^2)	$U(O)$ (Å^2)	$\mu_B(A)$	$\mu_B(B)$	χ^2	R_{wp} (%)
1	25	8.4811(3)	$Mn_{0.39}Fe_{0.61}$	$Mn_{0.82}Fe_{1.18}$	0.2589(2)	0.003(1)	0.003(1)	0.012(1)	−3.2(1)	2.5(1)	1.26	6.71
2	363	8.5131(3)	$Mn_{0.61}Fe_{0.39}$	$Mn_{0.52}Fe_{1.47}$	0.2597(2)	0.015(1)	0.009(7)	0.016(1)			1.28	9.00
3	485	8.5272(2)	$Mn_{0.62}Fe_{0.38}$	$Mn_{0.56}Fe_{1.43}$	0.2597(2)	0.009(5)	0.009(1)	0.020(1)			1.28	7.10
4	25	8.4884(2)	$Mn_{0.71}Fe_{0.29}$	$Mn_{0.50}Fe_{1.50}$	0.2606(2)	0.003[b]	0.005(1)	0.012(1)	−3.3(1)	2.3(1)	1.33	6.73

[a] Estimated standard uncertainties for the site occupancies are ±0.01.[25] [b] Fixed value.

°C, the magnetic ordering disappeared and only the nuclear scattering was observed, which is consistent with the observation of Curie temperature below 320 °C in general among these materials.[15] The refinement gives a cation distribution of 39% inversion with a formula of $Mn_{0.61}Fe_{0.39}(Mn_{0.52}Fe_{1.47})O_4$. As the temperature was raised to 485 °C, the cation distribution in the nanoparticles remained unchanged. When the sample was cooled back to 25 °C, the antiferromagnetic order was restored. The cation distribution showed a 29% inversion (Figure 4b), which is almost the same as that from the high-temperature measurements if the uncertainties in the data fits are considered.[25] The stable cation distribution after heating shows that an equilibrium state has been reached.

The initial 61% inversion for the cation distribution is due to the random occupancy of A and B sites by the cations following the 3/2 ratio of Fe to Mn in sample composition. As the nanoparticles are formed at room temperature, the thermal energy is too low to overcome the energy barrier to an ordered cation distribution. When the nanoparticles are heated, there is sufficient energy to enable the cations to diffuse and produce an equilibrium state of about 29% inversion. This change of cation distribution is consistent with the change of unit cell size. A relationship between unit cell size and cation distribution has been observed previously in bulk materials with cubic spinel structures. The inverse spinel has a smaller unit cell than its counterpart with normal cation occupancy.[4] This difference in unit cell size has been attributed to a shorter cation−anion bond for Fe^{3+} in the tetrahedral A sites compared to Fe^{3+} in the octahedral B sites, and to the possible change of Mn oxidation state.[4,10] In the nanoparticles with 29% inversion, the lattice constant is 8.4884(2) Å. In comparison, the lattice constant is 8.4811(3) Å in the nanoparticles with 61% inversion. In addition to the above change of inversion degree, such difference in unit cell size may also partially come from temperature-dependent variation of the Mn oxidation state.

Oxidation State. The oxidation state of Mn in Mn−Fe nanoparticles has been determined by EELS. In EELS studies, the inner-shell L ionization of transition metal usually displays sharp peaks at the near-edge region.[27] When the high-energy electron beam excites a 2p electron to a 3d orbital in a first-row transition metal, two sharp transitions are formed as L_3 and L_2 peaks. They are the electron transitions from the $2p^{3/2}$ electron state to $3d^{3/2}$ or $3d^{5/2}$ and from $2p^{1/2}$ to $3d^{3/2}$, respectively.[28] Systematic EELS studies have demonstrated that the change in the oxidation states of metal cations results in significant changes in the ratio of the peak intensities, $I(L_3)/I(L_2)$. Therefore, the intensities of peaks in EELS measurements can be used to identify the oxidation states.[29−31] EELS analysis

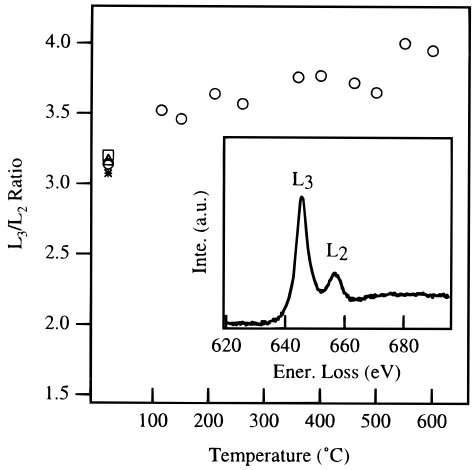

Figure 5. The plot of the peak intensity ratio of Mn L_3/L_2 following the temperature change. The intensity ratios were obtained from the EELS spectra of the sample nanoparticles recorded in situ at various temperatures. Five repeated measurements at 25 °C are shown and give consistent results. The inset shows a typical single-scattering EELS spectrum of Mn-$L_{2,3}$ ionization edges recorded at 25 °C.

of the oxidation state is carried out in reference to a working curve that has been established from the spectra acquired from standard samples with known oxidation states.[29]

The formation of Mn^{3+} cations may occur during the precipitation process since Mn^{2+} is easily oxidized in a highly basic solution.[32] EELS studies on the Mn−Fe spinel nanoparticles show that the oxidation state of Mn is a mixed +3 and +2 oxidation states in as-prepared nanoparticles. The Mn oxidation state changes to almost a pure +2 state as the nanoparticles are heated in a vacuum. For a typical EELS spectrum of Mn in the nanoparticles (Figure 5 inset), the ratio of the Mn L_3 and L_2 intensities increases with increasing temperature (Figure 5). Consistent results were obtained in five independent experiments. From various standard Mn compounds—MnO, Mn_3O_4, Mn_2O_3, and MnO_2—the Mn L_3/L_2 ratio is 2.26 for Mn^{3+} and 4.26 for Mn^{2+}. The percentages of the Mn^{3+} and Mn^{2+} cations in the samples can be determined based on the ratio of peak intensity relative to the L_3/L_2 ratios of Mn^{3+} and Mn^{2+}.[33,34] The results are plotted versus temperature in Figure 6. In as-prepared Mn−Fe spinel nanoparticles, Mn cations have both +3 and +2 states with about 50% for each. As the temperature increases, Mn^{3+} cations are slowly reduced to Mn^{2+}. When the temperature approaches 600 °C, virtually all Mn^{3+} cations in the nanoparticles are converted to Mn^{2+}. The change of the Mn oxidation state during the vacuum heating is the result of losing oxygen anions in the nanoparticles heated in a vacuum and the Mn^{3+} cations absorbing the extra

(27) Disko, M. M.; Ahn, C. C.; Fultz, B. *Transmission Electron Energy Loss Spectrometry in Materials Science*; The Minerals, Metals and Materials Society: Warrendale, PA, 1992.
(28) Krivanek, O. L.; Paterson, J. H. *Ultramicroscopy* **1990**, *32*, 313.
(29) Pearson, D. H.; Ahn, C. C.; Fultz, B. *Phys. Rev. B* **1993**, *47*, 8471.
(30) Kurata, H.; Colliex, C. *Phys. Rev. B* **1993**, *48*, 2102.
(31) Fortner, J. A.; Buck, E. C. *Appl. Phys. Lett.* **1996**, *68*, 3817.
(32) Liang, C. C. In *Encyclopedia of Electrochemistry of the Elements*; Bard, A. J., Ed.; Marcel Dekker: New York, 1973; Vol. 1, p 352.
(33) Wang, Z. L.; Yin, J. S.; Jiang, Y. D.; Zhang, J. *Appl. Phys. Lett.* **1997**, *70*, 3362.
(34) Wang, Z. L.; Yin, J. S.; Mo, W. D.; Zhang, Z. J. *J. Phys. Chem. B* **1997**, *101*, 6793.

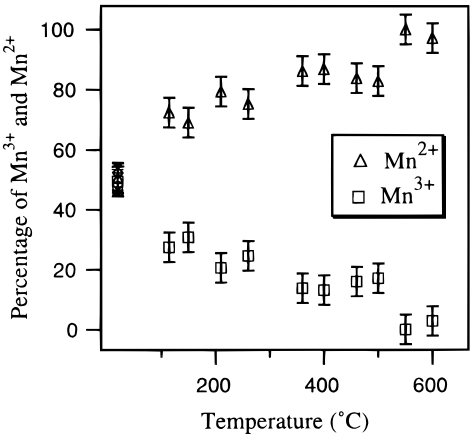

Figure 6. Calculated relative percentages of Mn^{2+} and Mn^{3+} based on the peak intensity ratios, showing the reduction process of Mn^{3+} to Mn^{2+} during the vacuum heating. Five repeated measurements at 25 °C are shown and give consistent results.

electrons to maintain the charge balance. This is consistent with the low oxygen contents in heat-treated samples estimated from ICP analysis by the increased percentage of Mn and Fe cation mass in the total sample mass. The EELS spectra of Fe^{3+} cations in the nanoparticles were also collected. However, the L_3/L_2 ratio for Fe shows little change. This implies that the oxidation state of Fe is very stable. This is understandable since Fe^{3+} is hard to reduce to Fe^{2+}. This also agrees with the unchanged isomer shift in the Mössbauer spectroscopy studies on Mn−Fe spinel and with other experiments.[12,13,35,36]

Conclusions

The cation distributions in the Mn−Fe spinel nanoparticles have been determined by neutron diffraction at various temperatures. These nanoparticles prepared by coprecipitation have a high degree of inversion with 61% of the A sites occupied by Fe as the result of cations randomly occupying A and B lattice sites. The cation distribution of the nanoparticles can be changed by the heat treatment in a vacuum. An equilibrium state of the cation distribution with a 29% inversion degree is higher than the usual 20% inversion in the Mn−Fe spinel prepared from solid-state reactions.[6] The Mn cations in as-prepared nanoparticles have both +3 and +2 oxidation states. The Mn^{3+} cations are irreversibly reduced to Mn^{2+} by heating the nanoparticles in a vacuum. Such crystal chemistry changes in Mn−Fe spinel nanoparticles should have a profound effect on the magnetic properties such as magnetic transition temperature. A decrease of about 50 °C in Mn−Fe spinel nanoparticles has been observed when the crystal chemistry of the particles is changed by annealing at 400 °C for 2 h.[37] In addition, these results clearly demonstrate that size effects on the magnetic properties of spinel nanoparticles have to be tightly connected with the crystal chemistry studies on these nanoparticles. The conclusion of particle size effect to Curie transition temperature from previous studies may not be valid since the crystal chemistry of Mn−Fe spinel nanoparticles in those studies has not been well defined. We believe that these results on the temperature dependence of the cation distribution and the oxidation state in the Mn−Fe spinel nanoparticles will be invaluable to the understanding of the magnetic properties of the spinel nanoparticles. Moreover, these results may provide rational approaches to facilitate the control of the magnetic properties in nanoparticles.

Acknowledgment. We thank Professor A. P. Wilkinson of Georgia Tech for his great help in the experiment and in the discussion, and we thank Dr. J. A. Fernandez-Baca of Oak Ridge National Laboratory for his help in neutron diffraction studies. Z.J.Z. gratefully acknowledges the financial support from Georgia Tech to initialize this research. The neutron diffraction studies were carried out at Oak Ridge National Laboratory, which is managed by Lockheed Martin Energy Research Corp. for the U.S. Department of Energy under contract number DE-AC0596OR22464.

JA973085L

(35) Lotgering, F. K. *Philips Res. Rep.* **1965**, *20*, 320.
(36) Sawatzky, G. A.; Woude, F. V. D.; Morrish, A. H. *Phys. Rev.* **1969**, *187*, 747.
(37) Liu, C.; Zhang, Z. J. Unpublished results.